When La-Co/ZrO_2 was calcined at 1123 K, $LaCoO_3$ perovskite or the like is formed in a highly dispersed state as fine particles or thin overlayers on the surface of ZrO_2 below the loading level of about 5 wt % (Figure 10, b and e).

The reaction between the substance (La-Co oxide) and ZrO_2 to form $La_2Zr_2O_7$ and Co_3O_4 occurred by the calcination above 1123 K and at and above the loading amount of 7.5 wt % (Figure 10, c and f). In these models, $La_2Zr_2O_7$ is formed in contact with ZrO_2 because the structure of pyrochlore $La_2Zr_2O_7$ is very close to that of tetragonal or cubic ZrO_2. The formation of $La_2Zr_2O_7$, Co_3O_4, and $LaCoO_3$ was observed in the XRD pattern of La-Co(5.1 wt %)/ZrO_2 calcined at 1373 K and the IR spectrum of La-Co(30 wt %)/ZrO_2 calcined at 1273 K, suggesting the model shown in Figure 10c.

Acknowledgment. The authors acknowledge JEOL for the EDX measurements. This work was supported in part by a Grant-in-Aid from the Ministry of Education, Science and Culture of Japan.

Registry No. La, 7439-91-0; Co, 7440-48-4; ZrO_2, 1314-23-4; NO, 10102-43-9; pyridine, 110-86-1.

Infrared Multiple Photon Dissociation of Acetone Radical Cation. An Enormous Isotope Effect with No Apparent Tunneling

Thomas H. Osterheld and John I. Brauman*

Contribution from the Department of Chemistry, Stanford University, Stanford, California 94305-5080. *Received February 18, 1992*

Abstract: Infrared multiple photon dissociation experiments on acetone cation and d_6-acetone cation indicate that the hydrogen atom abstraction resulting in methane loss does not involve tunneling. The large isotope effect arises from a competitive mechanism. Reaction thresholds and zero point vibrational energy differences indicate that the critical energy for methane loss is up to 0.9 kcal/mol below the threshold for loss of methyl radical in the unlabeled acetone cation system.

Reactions that may involve tunneling through potential barriers are an exciting area of study.[1] Tunneling is difficult to investigate experimentally, as discussed recently by Baer and co-workers;[2] classical barriers in the potential-energy surface cannot be measured experimentally, so that tunneling must be inferred from other methods such as isotope effect measurements. However, care must be taken to also consider changes in zero point vibrational energies (ZPVE) which give rise to "classical" isotope effects.

Recently it was proposed that methane elimination from acetone radical cation proceeds by a tunneling mechanism.[3] This reaction involves a hydrogen atom transfer step, and the metastable ion[4] of 1,1,1-d_3-acetone cation yields an enormous 70/1 preference for methane loss by hydrogen atom abstraction as opposed to deuterium atom abstraction[5] (eq 1).

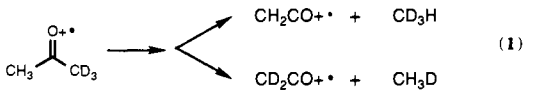

(1)

It would be surprising if this result arises from a "classical" isotope effect.[6] We show here, however, with infrared multiple photon (IRMP) dissociation[7-10] experiments on acetone cation and d_6-acetone cation, that methane loss does not occur by a tunneling mechanism.[11] The large apparent preference for abstraction of hydrogen arises from a phenomenon which we term a "competitive reaction isotope effect". Large isotope effects can be observed in metastable ions because they usually involve a narrow energy range near threshold. In this case, however, the large isotope effect arises from a competition between reactions and is not a consequence of the measurement technique or the range of energies populated by the experiment.

Systems that involve loose and tight transition states at similar energies may display competitive reaction isotope effects. In particular, we expect that this behavior will be encountered in other ion systems. Considerable evidence indicates that many low-energy reactions of gas-phase ions involve ion-neutral complexes.[12-19] Methane elimination from acetone cation belongs to a common class of reactions[15] (eq 2) which involve a bond cleavage to form an ion-neutral complex followed by a hydrogen atom abstraction by the neutral fragment. Inherent in this mechanism is the competition between a loose transition state (complete cleavage to separated products) and a tight transition state (hydrogen atom abstraction). Hydrogen atom abstraction can be observed if its

(1) Bell, R. P. *The Tunnel Effect in Chemistry*; Chapman and Hall Ltd.: New York, NY, 1980.
(2) Booze, J. A.; Weitzel, K.-M.; Baer, T. *J. Chem. Phys.* **1991**, *94*, 3649.
(3) Heinrich, N.; Louage, F.; Lifshitz, C.; Schwarz, H. *J. Am. Chem. Soc.* **1988**, *110*, 8183.
(4) Cooks, R. G.; Beynon, J. H.; Caprioli, R. M.; Lester, G. R. *Metastable Ions*; Elsevier Scientific Publishing Company: New York, NY, 1973.
(5) Lifshitz, C.; Tzidony, E. *Int. J. Mass. Spectrom. Ion Phys.* **1981**, *39*, 181.
(6) Recent experiments showing bond-specific reactivity display enormous isotope effects. (a) Bronikowski, M. J.; Simpson, W. R.; Girard, B.; Zare, R. N. *J. Chem. Phys.* **1991**, *95*, 8647. (b) Sinha, A.; Hsiao, M. C.; Crim, F. F. *J. Chem. Phys.* **1990**, *92*, 6334. (c) Sinha, A.; Hsiao, M. C.; Crim, F. F. *J. Chem. Phys.* **1991**, *94*, 4928.
(7) Lupo, D. W.; Quack, M. *Chem. Rev.* **1987**, *87*, 181.
(8) Quack, M. *J. Chem. Phys.* **1978**, *69*, 1282.
(9) Quack, M.; Seyfang, G. *J. Chem. Phys.* **1982**, *76*, 955.
(10) Dunbar, R. C. *J. Chem. Phys.* **1991**, *95*, 2537.
(11) Truhlar and co-workers have shown that many hydrogen atom transfer reactions involve aspects that can be attributed to tunneling. See: Garrett, B. C.; Truhlar, D. G.; Wagner, A. F.; Dunning, T. H., Jr. *J. Chem. Phys.* **1983**, *78*, 4400. Our experiments on acetone cation demonstrate that the barrier to hydrogen atom transfer lies below the endothermic threshold for methyl radical loss and that hydrogen atom transfer is not required to occur by tunneling *through* a potential barrier.
(12) Bowen, R. D. *Acc. Chem. Res.* **1991**, *24*, 364.
(13) Hammerum, S.; Audier, H. A. *J. Chem. Soc., Chem. Commun.* **1988**, 860.
(14) Lifshitz, C.; Rejwan, M.; Levin, I.; Peres, T. *Int. J. Mass. Spectrom. Ion Processes* **1988**, *84*, 271.
(15) McAdoo, D. J.; Hudson, C. E. *Int. J. Mass. Spectrom. Ion Processes* **1984**, *59*, 325.
(16) McAdoo, D. J. *Mass Spectrom. Rev.* **1988**, *7*, 363.
(17) Morton, T. H. *Tetrahedron* **1982**, *38*, 3195.
(18) Morton, T. H. *Org. Mass. Spectrom.* **1992**, *27*, 353.
(19) Longevialle, P.; Botter, R. *Org. Mass. Spectrom.* **1983**, *18*, 1.

0002-7863/92/1514-7158$03.00/0

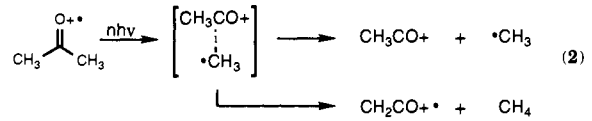

(2)

critical energy is lower than that of the complete cleavage. A higher critical energy for the abstraction reaction caused by normal ZPVE differences, as a result of isotopic substitution, can dramatically affect the branching between the two reactions.

While the direct interpretation is somewhat different from that used for normal isotope effects, competitive reaction isotope effect studies can be just as powerful. Extensive information can be obtained about potential-energy surfaces, especially when the effects are measured using IRMP dissociation.

Experimental Section

Materials. Acetone and d_6-acetone were purchased from Aldrich and used without further purification. 1,1,1-d_3-Acetone was synthesized by adding acetaldehyde to an ether solution of CD_3MgI to make the 1,1,1-d_3-2-propoxide and then adding an excess of benzaldehyde to oxidize the propoxide to 1,1,1-d_3-acetone. A normal Grignard workup was done using an initial wash with a NH_4Cl solution. 1,1,1-d_3-Acetone was separated from the ether by preparatory gas chromatography on a 20M Carbowax column at 80 °C. Samples were degassed by several freeze–pump–thaw cycles prior to introduction into the high-vacuum system.

Experiment. Ions were trapped, photolyzed, and detected with a Fourier transform mass spectrometer[20-22] (FT-MS) using the OMEGA data system from IonSpec. The system is equipped with both chirp excitation and the IonSpec impulse excitation.[23-25] We detected with impulse excitation because it gives more accurate isotope ratios and more stable signals. Ions were formed by electron impact ionization at low energies (about 15–20 eV), and then unwanted ions were ejected by standard notched ejection techniques. The ion of interest was then photolyzed by either a continuous wave (CW) or pulsed CO_2 laser followed by detection. Photolysis scans were compared to scans with the laser blocked to make sure we had mass balance and to correct for any background chemical ionization.

The FT-MS cell is contained in a home-built vacuum system capable of background pressures less than 1×10^{-8} Torr. Neutral pressures were measured with a nude ionization gauge. The pressures are not corrected; the absolute values are not critical to this study. Neutral ion precursors or reactant species enter through Varian sapphire leak valves. Laser light can enter the vacuum system through a Harshaw 50 mm × 3 mm KCl window[26] located at the front of the vacuum chamber and mounted on a conflat flange with Viton o-rings. The FT-MS uses an electromagnet capable of 1.4 T, but these experiments were done at 0.8 T to enable detection of low-mass ions.

The cell configuration is roughly a 1-in. cubic cell except that the front and rear plates (transmitter plates) are separated by $1^1/_2$ in. The cell plates are made from polished oxygen-free copper (OFHC). For some of these experiments we also used molybdenum cell plates. The rear cell plate is a commercial copper mirror from SPAWR Optical Research with a stated reflectivity of 99% at 10.6 μm. The front cell plate contains a 15/16-in. hole covered by a 95% transmitting copper mesh with 20 lines/in. These alterations allow laser light to pass into the cell and then be reflected collinearly back through the cell.

Pulsed laser photolysis was accomplished using the multimode output of a Lumonics TEA 103-2 CO_2 laser. The laser is line tunable using a grating element. We used a laser mixture containing nitrogen to achieve higher pulse energies. The temporal profile of the laser pulse (with nitrogen) consists of an initial high-intensity spike (about 80 ns fwhm) followed by a low-intensity tail extending for several microseconds (roughly 2 μs fwhm). The total energy is partitioned approximately equally between the spike and the tail. A Rofin 7400 photon drag detector and an Eltec 420-2 pyroelectric detector were used for the temporal profile measurements. A desired pulse energy is obtained by attenuating the laser beam with CaF_2 flats of varying thickness. The laser beam is weakly focused using a 10-m radius of curvature mirror located about 2.3 m from the FT-MS cell. An iris, located about 45 cm in front of the cell, provides the desired spot size. Intensity profile measurements with a pyroelectric detector indicate that this configuration gives a resonable "top hat" profile at the location of the cell. The profile contains intensity variations because the laser is operated multimode to achieve higher pulse energies.

Pulse energies were measured using a Scientech 365 power and energy meter with a Scientech 38-0102 volume absorbing disk calorimeter. The laser beam spot size was measured just in front of the KCl window to the vacuum chamber by burn spots on thermal paper. Reported fluences were calculated by taking the pulse energy divided by the spot size and then multiplying by 2. We multiply by 2 because the laser beam is reflected back on itself so it passes through the cell twice and effectively doubles the number of photons compared to a single pass.

The pulsed laser misfires up to 5% of the time. The percentage of misfires is fairly reproducible on any given day. For this reason we averaged at least 100 transients for any measurement so that the number of misfires would be reasonably constant between measurements.

Ions were also photolyzed using a home-built, grating-tuned, CW CO_2 laser. This laser provides about 10 W on the P(22) or P(24) lines of the 9.6-μm transition. Fluence can be controlled by changing the irradiation time with a Uniblitz shutter. Laser power was measured using an Optical Engineering 25-B power meter.

For both lasers, the laser wavelength was measured with an Optical Engineering 16-A CO_2 spectrum analyzer.

These experiments involved measuring branching ratios of ions with m/z 41–46. On several occasions during these experiments, we measured the isotope ratios for the CH_2Cl^+ (m/z 49 and 51) fragment from methylene chloride to ensure quantitative accuracy. We consistently obtained a value of 3.1 ± 0.1, which agrees with natural isotopic abundances.[27] We estimate that the branching ratios reported in this paper are accurate to ±5%.

Calculations. Ab initio molecular orbital calculations were performed using GAUSSIAN 90.[28] We started with the structures from the literature[3] and optimized with a 6-31G basis set to obtain harmonic vibrational frequencies of the labeled and unlabeled species of interest. We have only used these frequencies in our analysis and not the ab initio energetics. Optimizing with a different basis set had little effect, so that the previous ab initio study[3] can be consulted for structures. The frequencies were scaled by a factor[29] of 0.9 to obtain estimates for the ZPVE of relevant species.

Table I. Branching Ratios from Pulsed Laser Photolysis of Acetone Cation and d_6-Acetone Cation[a]

fluence	CH_3/CH_4	CD_3/CD_4	% yield
1.02		4.0 ± 0.3	4.6
1.07	4.5 ± 0.5		3.7
1.27		4.7 ± 0.2	6.4
1.38	4.7 ± 0.3		5.2
1.52		5.3 ± 0.1	9.1

[a] Fluences are in J/cm².

Results

At low energies, acetone cation can lose either methane or methyl radical[3,5,30-32] (eq 2). These are the only reactions energetically accessible with IRMP dissociation using our lasers. IRMP dissociation was effected using the P(22) or P(24) lines of the 9.6-μm transition. These lines correspond to 1047 and 1045 cm^{-1} and are the wavelengths at which acetone cation absorbs most strongly. At these wavelengths, d_6-acetone cation absorbs more strongly than the unlabeled acetone cation and d_3-acetone cation absorbs less strongly. The total abundance of ions was the same in the "light on" and "light off" experiments. In other words, the

(20) Marshall, A. G.; Verdun, F. R. *Fourier Transforms in NMR, Optical, and Mass Spectrometry: A User's Handbook*; Elsevier: New York, 1990.
(21) Marshall, A. G.; Grosshans, P. B. *Anal. Chem.* **1991**, *63*, 215A.
(22) Grosshans, P. B.; Shields, P. J.; Marshall, A. G. *J. Chem. Phys.* **1991**, *94*, 5341.
(23) McIver, R. T., Jr.; Baykut, G.; Hunter, R. L. *Int. J. Mass. Spectrom. Ion Processes* **1989**, *89*, 343.
(24) McIver, R. T., Jr.; Hunter, R. L.; Baykut, G. *Anal. Chem.* **1989**, *61*, 489.
(25) McIver, R. T., Jr.; Hunter, R. L.; Baykut, G. *Rev. Sci. Instrum.* **1989**, *60*, 400.
(26) The 3-mm windows last significantly longer than the 6-mm windows.
(27) McLafferty, F. W. *Interpretation of Mass Spectra*, 3rd ed.; University Science Books: Mill Valley, CA, 1980.
(28) Frisch, M. J.; Head-Gordon, M.; Trucks, G. W.; Foresman, J. B.; Schlegel, H. B.; Raghavachari, K.; Robb, M. A.; Binkley, J. S.; Gonzalez, C.; Defrees, D. J.; Fox, D. J.; Whiteside, R. A.; Seeger, R.; Melius, C. F.; Baker, J.; Martin, R. L.; Kahn, L. R.; Stewart, J. J. P.; Topiol, S.; Pople, J. A. *GAUSSIAN 90*; Gaussian, Inc.: Pittsburgh, PA, 1990.
(29) Hehre, W. J.; Radom, L.; Schleyer, P. v. R.; Pople, J. A. *Ab Initio Molecular Orbital Theory*; Wiley: New York, NY, 1986.
(30) Traeger, J. C.; Hudson, C. E.; McAdoo, D. J. *J. Phys. Chem.* **1988**, *92*, 1519.
(31) McAdoo, D. J.; Witiak, D. N. *J. Chem. Soc., Perkin Trans. 2* **1981**, 770.
(32) Derrick, P. J.; Hammerum, S. *Can. J. Chem.* **1986**, *64*, 1957.

sum of the product ion abundances and the unreacted parent ion abundance, measured in the photolysis experiments, was the same as the unreacted parent ion abundance when the laser was blocked. This was true for both the CW and pulsed lasers.

CW Laser Photolysis. The branching ratio for the CW laser photolysis of h_6-acetone cation = $(CH_3)/(CH_4)$ = 2.4 ± 0.1 (0.04). The branching ratio for d_6-acetone cation = $(CD_3)/(CD_4)$ = 2.2 ± 0.1 (0.03). The reported errors are our estimates of the accuracy of the branching ratios while the numbers in parentheses are the standard deviations of at least five measurements. Each measurement involves averaging 500 transients. The ions were irradiated for times ranging from 260 to 320 ms. The amount of irradiation did not appear to affect the branching ratios. These experiments were repeated on other days, and we obtained values within the error of these values.

Pulsed Laser Photolysis. Table I lists branching ratios as a function of fluence (at constant pulse length) for the pulsed laser photolysis of acetone cation and d_6-acetone cation. It is apparent that the branching ratios are essentially the same for acetone cation and d_6-acetone cation, at a given fluence (at least at these low fluences). This means that the amount of methane loss is essentially the same for acetone cation and d_6-acetone cation. Increasing the fluence increases the photon intensity.[33] The error estimates are the standard deviations of three to five measurements. Each measurement involves averaging 100–500 transients. More transients are averaged for the lower fluence measurements. The branching ratio does not depend on the number of transients averaged.

Background Reactivity. We want to measure the amount of CH_3CO^+ and $CH_2CO^{\bullet+}$ (or the corresponding ions for the labeled species) produced by IRMP dissociation of acetone cation. The acetone cation system contains background reactions, which must be controlled to ensure accurate branching ratio measurements. Throughout the background reactivity section, we use the unlabeled acetone cation as an example. The issues are the same for the labeled species and simply involve isotopomers of the ions discussed.

IRMP experiments on CH_3CO^+ (and CD_3CO^+) formed by electron impact indicate that CH_3CO^+ does not undergo IRMP dissociation. Although we could not generate enough $CH_2CO^{\bullet+}$ to test if it undergoes IRMP dissociation, photolysis of acetone cation did not generate any ion lower in mass than $CH_2CO^{\bullet+}$. These experiments indicate that we do not need to worry about secondary photochemistry giving product loss or dissociating CH_3CO^+ to give $CH_2CO^{\bullet+}$ + H•.

Acetone cation reacts with its neutral parent[34] to give products at higher masses: protonated acetone cation (M + 1) and an ion corresponding to M + CH_3CO (eq 3). These species can also

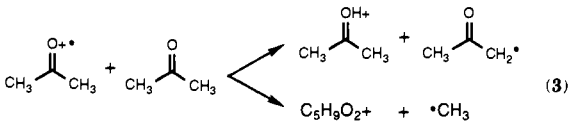

(3)

undergo IRMP dissociation to give CH_3CO^+. Acetone cation also reacts with its neutral parent to give products at lower masses (eq 4). Control of these issues is discussed in two separate sections,

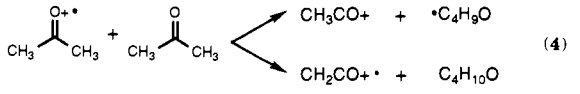

(4)

one for the pulsed laser and one for the CW laser.

Pulsed Laser. To minimize background reactions we conducted the experiments at lower pressures (1–5 × 10^{-8} Torr). Acetone cation was isolated by standard notched ejection techniques. CH_3CO^+ and $CH_2CO^{\bullet+}$, which may have formed by background reactions, were ejected immediately (about 5 ms) before the laser pulse. The products were detected within 5–10 ms after the laser pulse. From the last ejection to the time of detection (about 15 ms in this case), a small amount of CH_3CO^+ and $CH_2CO^{\bullet+}$ will have formed by background reactions. To measure this, we took scans with the laser blocked and observed how much CH_3CO^+ and $CH_2CO^{\bullet+}$ were formed. The amount was converted to a fraction of total ions and then used to correct the abundances of CH_3CO^+ and $CH_2CO^{\bullet+}$ for experiments with the laser light entering the cell. This correction must be made because the ions from background reactions predominantly give CH_3CO^+ but little $CH_2CO^{\bullet+}$. Very little of the M + 1 or M + CH_3CO ions form during the short time between their ejection and the detection of products, so we do not need to worry about photochemistry of these species with the pulsed laser experiments.

CW Laser. These experiments were conducted at the lowest pressures (0.5–2 × 10^{-8} Torr), to minimize background reactions as much as possible. CH_3CO^+ and $CH_2CO^{\bullet+}$ were ejected immediately before laser irradiation, and were detected as soon as possible after laser irradiation. CH_3CO^+ and $CH_2CO^{\bullet+}$ abundances were corrected with the same method used in the pulsed laser experiments. Acetone cation must be irradiated for long times (260–320 ms). In that time, significant amounts of the M + 1 ion and M + CH_3CO ion can form. These ions were continuously ejected during the laser pulse so that they cannot also undergo IRMP dissociation. We use an external box to mix the frequency provided by the IonSpec data system with a frequency provided by a Hewlett-Packard 3325A function generator to permit two continuous ejections at the same time.

With the CW laser experiment we also must consider the possibility that the photoproducts may undergo reaction before detection. In this case we must assume that both CH_3CO^+ and $CH_2CO^{\bullet+}$ react with acetone at the same rate so that branching ratios will not be affected. This is probably not an unreasonable assumption.[35] Even if CH_3CO^+ and $CH_2CO^{\bullet+}$ react at unequal rates, the experiment is done at low pressures and most of the photoproduct is only present toward the end of laser irradiation so any error should be minimal. Support for this argument comes from the observation that the branching ratio does not depend on the length of irradiation time.

***d*$_3$-Acetone Cation.** We also studied the IRMP dissociation of 1,1,1-d_3-acetone cation (eq 5). The measurement of interest

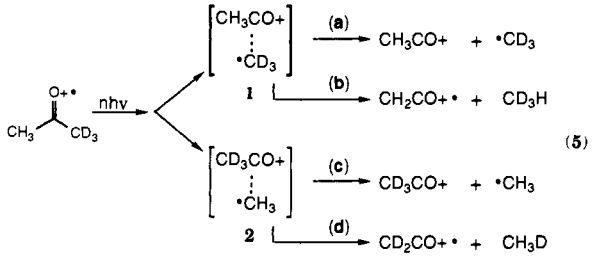

(5)

involves photolysis with the CW laser. We obtain a branching ratio for methane loss of CD_3H/CH_3D > 8/1. This ratio could be significantly larger than 8/1 (i.e., as much as 70/1 as observed in the metastable ion experiment[5]), but we cannot measure it more accurately because of an impurity (vide infra). In any event, the ratio is large. If we assume that essentially no CH_3D loss occurs, we obtain branching fractions for $CH_3/CD_3/CD_3H$ which are 0.61 ± 0.02/0.21 ± 0.02/0.18 ± 0.02. The error estimates come from relative differences in measurements from different days and different samples. The precision for any series of measurements is better than the error estimates.

This experiment was significantly more difficult than the acetone and d_6-acetone cation experiments. The d_3-acetone cation absorbs substantially more weakly than either acetone cation or

(33) We actually want to measure branching ratios as a function of intensity, but because the laser pulse has two components, it is hard to define the intensity. For this reason we simply report the branching ratios as a function of fluence and realize that any changes in branching ratios are a result of intensity changes. Two laser pulses with the same fluence should also have essentially the same intensity at a given time during the laser pulse.

(34) Diekman, J.; MacLeod, J. K.; Djerassi, C.; Baldeschwieler, J. D. *J. Am. Chem. Soc.* **1969**, *91*, 2069.

(35) Vogt, J.; Williamson, A. D.; Beauchamp, J. L. *J. Am. Chem. Soc.* **1978**, *100*, 3478.

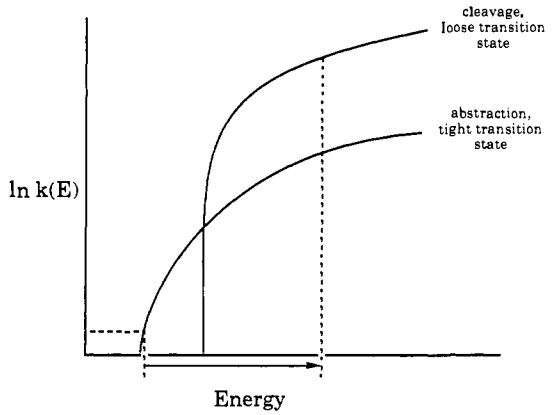

Figure 1. Graphical representation of the dissociation energy range (denoted by the arrow), after IRMP activation with a CW laser, for a lower energy tight transition state competing with a loose transition state. The x-axis is energy, and the y-axis gives the rate constant. Note that the x-axis does not start at zero energy.

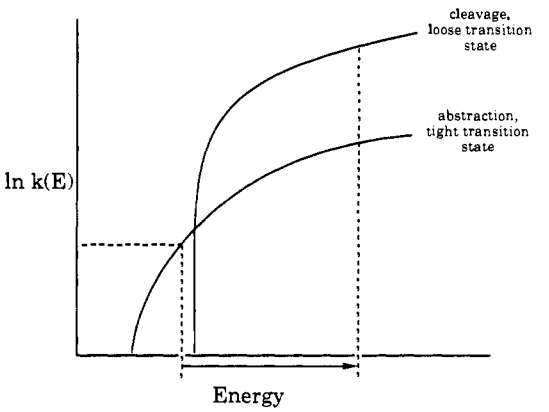

Figure 2. Graphical representation of the dissociation energy range (denoted by the arrow), after IRMP activation with a pulsed laser, for a lower energy tight transition state competing with a loose transition state. The x-axis is energy, and the y-axis gives the rate constant. Note that the x-axis does not start at zero energy.

d_6-acetone cation. We had to average 1000 scans to obtain reasonable (although small) signals of photoproduct. Our d_3-acetone cation contained about 13% d_2 impurity and 10% d_1 impurity as well as a small amount of ether from the synthesis. All impurity ions were ejected before laser irradiation. Experiments were done at $1-2 \times 10^{-8}$ Torr, and the M + 1 ion was continuously ejected during the laser pulse. From the photochemistry experiments, it is clear that our sample contained an isomerized 1,1,3-d_3-acetone impurity (ions other than m/z 61 were ejected before laser irradiation). The parent ion of this species obviously has the same mass as 1,1,1-d_3-acetone cation so it cannot be detected directly. However, our sample gives a photoproduct at m/z 45 (CD_2HCO^+) which cannot come from 1,1,1-d_3-acetone. This ion is also observed on electron impact but could come from the d_2 impurity in the electron impact experiment. We estimate the abundance of the impurity to be about 10%, assuming it absorbs the same as 1,1,1-d_3-acetone cation. Unfortunately, this impurity complicates measuring a branching ratio for methane loss (CD_3H/CH_3D) because the ion corresponding to CH_3D loss is $CD_2CO^{\cdot+}$ (m/z 44.0231) and the isomerized impurity can give CDH_2CO^+ (m/z 44.0247) by a facile reaction. Irradiation of our d_3-acetone cation sample gives a small peak at m/z 44.0247. We were unable to do the experiment at sufficient resolution to discern if this peak had a smaller component at m/z 44.0231. We give a branching ratio of $CD_3H/CH_3D > 8/1$ based on an estimate of the biggest possible peak of $CD_2CO^{\cdot+}$, which would not be resolved from the CDH_2CO^+ peak. We did not pursue trying to remove the isomerized impurity because we suspect that isomerization can occur on the metal surface of the foreline, a problem which is unavoidable with our present system.

Experimental Considerations

IRMP dissociation involves ions which dissociate after sequentially absorbing infrared photons. We use a CO_2 laser so the energy increment (energy of one photon) is about 3 kcal/mol, and therefore the ions dissociate over an energy range of at least 3 kcal/mol. The activation process involves energy pumping, which in most cases occurs at a steady-state rate dependent on the intensity. Reaction starts to occur at the energy where the reaction rate competes with the pumping rate. Photolysis with a CW laser involves a pumping rate[36] of about 10 s^{-1} so that the energy range for dissociation starts at the point where the lowest energy reaction has achieved a rate of 10 s^{-1}. Figure 1 uses $k(E)$ curves to show the dissociation energy range (from IRMP with a CW laser) for an abstraction with a tight transition state competing with a cleavage with a loose transition state. The horizontal line in Figure 1 indicates the pumping rate. The point where the horizontal line first meets a $k(E)$ curve controls the start of the energy range for dissociation. The energy range for dissociation is indicated by the two vertical dashed lines and encompasses at least the energy of one photon (3 kcal/mol). Photolysis with the pulsed laser involves pumping rates of 10^4-10^6 s^{-1}, and some reactions (especially abstractions or rearrangements) may not achieve this rate except at energies significantly above threshold. Pulsed laser photolysis, therefore, can shift the energy range of dissociation to higher energies because an ion energized slightly above the reaction threshold will absorb another photon if its reaction rate does not compete with the pumping rate. Figure 2 uses $k(E)$ curves to show the dissociation energy range (from IRMP with a pulsed laser) for an abstraction competing with a cleavage. In the case of the pulsed laser the energy range may be broader than the 3 kcal/mol range depicted in Figure 2.

Several conclusions can be drawn from these arguments and inspection of Figures 1 and 2. Both abstractions and cleavages can be observed in IRMP dissociation. The energy range of reaction is at least 3 kcal/mol regardless of the competition, so useful branching ratios between fast and slow reactions can be obtained. Comparisons can be made between CW laser photolysis and pulsed laser photolysis to observe energy or pumping rate dependences. As with metastable ions, abstractions may only be observed over a limited energy range if a cleavage occurs at higher energies.

The low-energy reactions of acetone cation provide a perfect example of these considerations. The metastable ion of acetone cation gives only methane loss[3,5,30-32] (abstraction). Higher energy collisional activation and electron impact show methyl radical loss[3,5,30-32,37] (cleavage) dominating the methane loss. IRMP dissociation of acetone cation with a CW laser gives a branching ratio for methyl loss to methane loss of 2.4/1. IRMP dissociation at higher energies with the pulsed laser gives a branching ratio of 4.5/1 or larger because methyl loss dominates at higher energies.

Discussion

The large branching ratio of CD_3H/CH_3D loss from 1,1,1-d_3-acetone cation suggests a tunneling mechanism because it appears surprisingly large for a classical isotope effect. In addition, ab initio calculations of the potential surface indicate that methane loss should occur by tunneling.[3] However, IRMP dissociation of acetone cation and d_6-acetone cation is inconsistent with a tunneling mechanism. We believe the large branching ratio from the d_3 species arises because of a facile competitive reaction (methyl loss) that limits methane loss.[38] Since the reaction pathways involve such small differences in energy, we would not be surprised if the ab initio calculations do not quantitatively reproduce the energetics.

(36) This value comes from a fluence dependence study of acetone cation photolysis. See refs 7–9.

(37) Qian, K.; Shukla, A.; Futrell, J. *J. Chem. Phys.* **1990**, *92*, 5988.

(38) It was pointed out in ref 3 that a competitive mechanism can give large isotope effects.

Consider eq 5. 1,1,1-d_3-Acetone cation can break the bond to the CD_3• group or the CH_3• group and form an ion–neutral complex. The complex with the CD_3• fragment may abstract a hydrogen atom because this process is lower in energy. The complex with the CH_3• fragment does not abstract a deuterium atom because *the process is not lower in energy*. The ratio of CD_3H loss to CH_3D loss is large because CH_3D loss cannot compete with CH_3• loss.

Classical isotope effects arise from ZPVE differences. For example, transfer of a deuterium atom usually has a higher critical energy than transfer of a hydrogen atom due to the lower ZPVE of an X–D bond and the relative loss of the ZPVE of the bond in the transition state. This gives rise to a "normal" primary isotope effect.[39] The rate of any reaction at an energy ϵ above the critical energy depends on the ratio of the sum of states of the transition state to the density of states in the energized reactant. For many reactions involving deuterium atom versus hydrogen atom transfer, this ratio is essentially the same at a given ϵ above the critical energy. Thus, the rate for deuterium atom transfer should be the same as for hydrogen atom transfer at a given energy above their respective thresholds.

Isotope effects caused by tunneling arise because deuterium is almost twice as heavy as hydrogen; deuterium thus has a much lower tunneling probability owing to the increased reduced mass in the reaction coordinate. Even in the absence of ZPVE differences, deuterium will react much more slowly than hydrogen. In other words, if tunneling is involved, deuterium should transfer at a rate significantly slower than hydrogen at a given energy above their respective thresholds.

d_6-Acetone cation can lose CD_4 only by transferring a deuterium atom. If tunneling is important, CD_4 loss will be suppressed (because the rates will be slower at a given energy) while a nontunneling mechanism would only change the threshold energy for CD_4 loss. By using IRMP dissociation we can compare methane loss from d_6- and h_6-acetone cation using methyl loss as a reference. Thus, IRMP dissociation gives both methane and methyl loss, and we can compare the relative abundances of the two pathways for the labeled and unlabeled species (eq 2).

Three major observations arise from the IRMP dissociation studies of d_6- and h_6-acetone cation: (1) CW laser photolysis gives the same amount of methane loss from both species. (2) Pulsed laser photolysis gives the same amount of methane loss from both species. (3) Pulsed laser photolysis gives less methane loss than CW laser photolysis.

These three observations give the following direct interpretations: (1) Both species give the same relative amount of methane loss over a 3 kcal/mol energy range starting near threshold (Figure 1). (2) In the pulsed laser photolysis, the reaction rate near threshold (for methane loss) is slower than the pumping rate, but at some point above threshold the reaction rate competes with the pumping rate. Methane loss occurs over the energy range which starts at the energy where the rate for methane loss competes with the pumping rate and ends at the energy where methyl loss dominates methane loss (Figure 2). (3) Even though methane loss only occurs when its reaction rate competes with the pumping rate, pulsed laser photolysis gives the same amount of methane loss from the labeled and unlabeled species.

The same amount of CD_4 loss as CH_4 loss in the pulsed laser photolysis is not consistent with a tunneling mechanism. For the CW laser experiments, it is possible that the pumping rates are slower than reaction rates, so that the branching ratios mostly reflect thermodynamic differences between the two reactions. However, we know that the branching ratios from the pulsed laser experiments do reflect reaction rates because they increase (less methane loss) compared to the CW laser experiments. This means that the CD_4 loss and CH_4 loss reactions achieve comparable rates at about the same relative energy. For a tunneling mechanism the rate-limiting step would involve tunneling through the barrier.

(39) If the transfer occurs from a CD_3 group, then it will also involve a secondary isotope effect (in the same direction) due to the hybridization change.

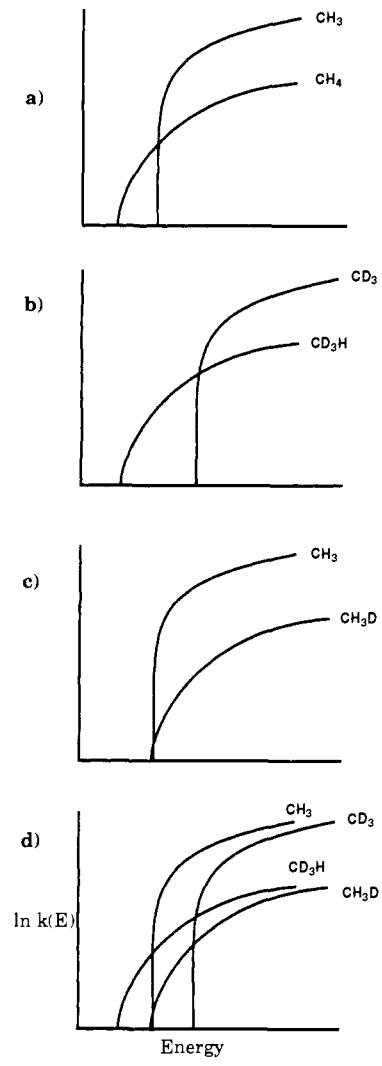

Figure 3. Rate constant (y-axis) versus energy (x-axis) curves for methyl loss and methane from the following: (a) acetone cation, (b) intermediate **1** in eq 5, (c) intermediate **2** in eq 5, and (d) 1,1,1-d_3-acetone cation. Note that the x-axis does not start at zero energy.

Table II. Critical Energies[a] Based on Molecular Beam Experiments[b] and Branching Ratios from CW Laser Experiments[c]

			critical energies
$CH_3C(=O^{\bullet+})CH_3$	$\xrightarrow{nh\nu}$	$\rightarrow CH_3CO^+ + {}^{\bullet}CH_3$	20
		$\rightarrow CH_2CO^{\bullet+} + CH_4$	19.12
$CD_3C(=O^{\bullet+})CD_3$	$\xrightarrow{nh\nu}$	$\rightarrow CD_3CO^+ + {}^{\bullet}CD_3$	20.9
		$\rightarrow CD_2CO^{\bullet+} + CD_4$	19.97

[a] In kcal/mol. [b] For loss of methyl radical (see ref 48). [c] For loss of methane (see Appendix).

Yet tunneling of a deuterium atom would only compete with the pumping rate at energies significantly higher than those for hydrogen,[40] so that CD_4 loss could not achieve a rate comparable to CH_4 loss. A tunneling mechanism is not consistent with the observation that d_6-acetone cation gives the same amount of methane loss as h_6-acetone cation in the pulsed laser photolysis.[41] Therefore, methane loss cannot occur by tunneling.[42]

(40) About 1.4 kcal/mol higher according to the tunneling scheme in ref 3. Lifshitz, C. Personal communication.

(41) The fact that d_6-acetone cation absorbs more strongly than h_6-acetone cation means that for an equal fluence some of the d_6-acetone cations may react at higher energies. This actually strengthens the argument against a tunneling mechanism.

Table III. Comparison of Critical Energies[a] for Eq 5

		predicted crit energy[b]	crit energy from branching fractions[c]	calcd rel energy[d]	calcd rel energy plus reference
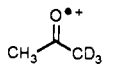	→ $CH_3CO^+ + {}^\bullet CD_3$	20.9		1.07	21.07
	→ $CD_3CO^+ + {}^\bullet CH_3$	20	20	0.10	20.10
	→ $CD_2CO^{\bullet+} + CH_3D$	19.97	~20	0.13	20.13
	→ $CH_2CO^{\bullet+} + CD_3H$	19.12	19.46	−0.58	19.42

[a] In kcal/mol. [b] Critical energies based on estimates of isotope effects using experiments in Table II. [c] Critical energies using analysis in Appendix and assuming $CH_3^\bullet$ loss occurs at 20.0 kcal/mol. [d] Relative energies with respect to methyl radical loss from h_6-acetone cation occurring at 20.0 kcal/mol (methane loss 0.88 kcal/mol lower). Relative energies obtained using ZPVE differences from ab initio frequencies.

These results are, however, completely consistent with a nontunneling mechanism. Methane loss is lower in energy than methyl loss[43] by roughly 0.5–1 kcal/mol (for the unlabeled species); Figure 3a graphically shows the $k(E)$ curves for the acetone cation dissociations. The energy difference between the two pathways is essentially the same for d_6-acetone cation because normal ZPVE differences raise the thresholds for both pathways. Specifically, a secondary isotope effect raises the threshold for $CD_3^\bullet$ loss, and a primary isotope effect (as well as a secondary isotope effect on the hydrogen transfer) raises the threshold for CD_4 loss by about the same amount. The net result is that the energy difference between the thresholds for the two pathways is essentially the same for both d_6- and h_6-acetone cation (CD_4 loss is still lower in energy than $CD_3^\bullet$ loss).

Consider the possible isotope effects for intermediate **1** in eq 5. A secondary isotope effect for loss of $CD_3^\bullet$ will shift the $k(E)$ curve for cleavage to higher energies.[44] The hydrogen atom abstraction will not have a primary isotope effect, so its $k(E)$ curve should not shift significantly when compared to CH_4 loss from unlabeled acetone cation.[45] The shifts in the $k(E)$ curves due to these isotope effects are shown in Figure 3b (ignoring intermediate **2**). The critical energies in Figure 3 can be compared between graphs because they all have a common energy scale.

Consider the possible isotope effects for intermediate **2**. There should be no significant isotope effect on the cleavage reaction, so its $k(E)$ curve should not be affected.[46] However, a primary isotope effect and a secondary isotope effect will shift the $k(E)$ curve for abstraction to higher energies. The secondary isotope effect on the abstraction arises because sp^2-hybridized C–D bonds[44] in $CD_2CO^{\bullet+}$ are formed. The shifts of the $k(E)$ curves from these isotope effects are shown in Figure 3c (ignoring intermediate **1**).

Because deuterium atom abstraction is not lower in energy and has a much lower A-factor than the cleavage to lose $CH_3^\bullet$, deuterium abstraction is slower than $CH_3^\bullet$ loss at all energies and therefore very little CH_3D loss is observed.[47] The $k(E)$ curves for all of the low-energy dissociations of 1,1,1-d_3-acetone cation are given in Figure 3d. CD_3H loss is observed because it has the lowest critical energy of all of the reactions.

These analyses can be done more quantitatively. We make an estimate of the energy difference between the two pathways using the branching ratio obtained from the CW laser photolysis of acetone cation (see Appendix). We then make estimates of the magnitude of the isotope effects in two different ways. We use appearance energies and branching ratios for d_6- and h_6-acetone cation to predict the thresholds for 1,1,1-d_3-acetone cation. We also use vibrational frequencies from ab initio calculations to estimate the ZPVE of each species in order to predict the thresholds.

Molecular beam photoionization experiments on acetone give a critical energy for methyl loss of 19.5 kcal/mol or higher.[48] For discussion purposes, we assume a critical energy of 20 kcal/mol. We calculate that the threshold for methane loss is 0.88 kcal/mol lower in energy based on the branching ratio. Molecular beam photoionization experiments on d_6-acetone give a critical energy for methyl loss that is 0.9 kcal/mol higher than that of the unlabeled species.[48] We calculate that methane loss is 0.93 kcal/mol lower in energy. These reaction thresholds are summarized in Table II.

We can estimate the isotope effects by comparing the dissociation of h_6- and d_6-acetone cation. $CD_3^\bullet$ loss is about 0.9 kcal/mol higher in energy (20.9 − 20 = 0.9). Abstraction of a deuterium atom is 0.85 kcal/mol higher in energy (19.97 − 19.12 = 0.85). We use these values to give the predicted thresholds for 1,1,1-d_3-acetone cation, shown in Table III. Table III also gives the threshold estimates for CH_3D loss and CD_3H loss based on the branching fractions (using the analysis in the Appendix and assuming that CH_3 loss occurs at 20 kcal/mol). These thresholds support the $k(E)$ curves that we proposed (Figure 3). The predicted thresholds agree well with those from the branching fractions. The branching fraction gives a higher threshold for CD_3H loss, because the predicted number did not include the contribution of a secondary isotope effect arising from the cleavage of a $CD_3^\bullet$ group in the first step of the reaction.

The thresholds were also predicted by using the ZPVE of acetone cation, the ZPVE of the transition state for methane loss, the ZPVE of $CH_3^\bullet$ plus CH_3CO^+, and the ZPVE of CH_4 plus $CH_2CO^{\bullet+}$ all obtained from ab initio calculations. We also obtained the ZPVE for their labeled counterparts in the 1,1,1-d_3-acetone cation system. We have assumed (as is usual) that the transition state for methyl loss looks much like the separated products and has the same vibrational frequencies as the separated products. Using the thresholds for unlabeled acetone cation (Table II), we subtract out the ZPVE contribution to each species to obtain the electronic thresholds for each channel. In doing this, we are using the ab initio frequencies but we are not using the ab initio energies. We can then add in the ZPVE contributions for the labeled species to predict the energy thresholds for 1,1,1-d_3-acetone cation. The predicted thresholds are given in Table III. These thresholds also agree well with the $k(E)$ curves

(42) The ZPVE differences might be such that methane loss could occur over a larger energy range for d_6-acetone cation and/or the transition state for methane loss, in the d_6 species, might be lower in energy when compared to methyl loss. However, frequency estimates of the relevant species (vide infra) indicate that the transition state for d_6-acetone cation would be at about the same energy as for h_6-acetone cation when compared to methyl loss. These frequency estimates also indicate that the energy range for methane loss from the d_6 species could be at most about 0.2–0.3 kcal/mol larger. This would not be enough to give the same amount of methane loss from both d_6- and h_6-acetone cations (see refs 3 and 40).

(43) Although appearance energy measurements cannot distinguish if methane loss is lower in energy than methyl loss, several pieces of evidence support this proposal. Methane loss is observed in the metastable ion spectrum, but at higher energies it is dominated by methyl loss. The IRMP results show that methane loss cannot occur by tunneling. For methane loss to be observed it must have a lower energy threshold.

(44) Streitweiser, A.; Jagow, R. H.; Fahey, R. C.; Suzuki, S. *J. Am. Chem. Soc.* **1958**, *80*, 2326.

(45) Throughout the discussion on isotope effects we assume that the major ZPVE differences for methane elimination stem from the changes in bonding due to the hydrogen atom abstraction step. We assume that the isotope effect on the bond cleavage in formation of the complex is not as important. Consistent with this, 1,1,1-d_3-acetone cation gives CD_3H loss and not CH_3D loss even though the ZPVE differences influencing formation of the complexes would favor CH_3D loss.

(46) This proposal is borne out by the ZPVE differences obtained from the ab initio calculations.

(47) Lifshitz, C.; Shapiro, M. *J. Chem. Phys.* **1967**, *46*, 4912.

(48) Trott, W. M.; Blais, N. C.; Walters, E. A. *J. Chem. Phys.* **1978**, *69*, 3150.

in Figure 3 and the previous estimates based on the branching ratios.

Conclusions

We have shown that methane loss from acetone cation does not occur by a tunneling mechanism in the IRMP dissociation.[11] The large isotope effects observed in this system appear to arise from competitive reaction isotope effects. Using IRMP branching ratios we were able to estimate the energy difference between methane loss and methyl loss as well as ZPVE differences associated with isotopic substitution. These estimates agree with ZPVE differences obtained with frequencies from ab initio calculations.

Competitive reaction isotope effects should occur in other gas phase ion reactions. A general mechanism involving ion-neutral complexes and hydrogen atom abstraction has arisen for many low-energy rearrangements[12-19] (eq 2). ZPVE differences due to isotopic substitution can raise the energy for the abstraction so that it is not lower in energy than the complex simply dissociating. We believe that several previous studies can be understood by considering these issues.[16,30,49-52]

Acknowledgment. We are grateful to the National Science Foundation for support of this work. We thank Professors Helmut Schwarz and Chava Lifshitz for insights and helpful discussions. We are grateful to Professor Robert McIver and Dr. Richard Hunter of IonSpec for considerable technical help. T.H.O. gratefully acknowledges graduate fellowship support from the W. R. Grace Foundation.

Appendix. Estimates of Reaction Threshold Differences Using Branching Ratios from CW Laser Photolysis

We assume that the energy range goes from threshold to 2.99 kcal/mol above threshold. The energy equivalent of P(22) and P(24) photons from the 9.6-μm transition is 2.99 kcal/mol. The range starts at threshold because methane loss should be faster than the 10-s^{-1} pumping rate essentially at threshold.

We assume a square (uniform) energy distribution over the 2.99 kcal/mol range. The energy distribution after electron impact ranges from the ionization potential to the lowest energy threshold and contains resonances which are observed in the photoelectron spectrum. Under irradiation the ions undergo transitions up and down the vibrational ladder due to absorption and stimulated emission, which should help to "smear" out the resonances in the distribution. The resonances also tend to be much broader than 2.99 kcal/mol. Other experiments in our laboratory support this square energy distribution proposal.[53]

Given these assumptions, the difference between the methane and methyl loss thresholds comes from X in the following equation:

$$\text{branching ratio} = \frac{2.99 - X}{X} \qquad (6)$$

For example, acetone cation has a branching ratio of 2.4, which gives an energy range for methane loss of 0.88 kcal/mol. Methyl loss is more facile than methane loss and should dominate at an energy slightly above the methyl loss threshold.[3,5,30-32,37] Equation 6 assumes that an ion will eliminate methane below the methyl loss threshold and not above. While this assumption is not strictly true, it should be reasonable because little methane loss is observed in pulsed laser photolysis at high fluences.[54]

Registry No. $H_3CCOCH_3^{\bullet+}$, 34484-11-2; D_2, 7782-39-0; H_2, 1333-74-0; CH_4, 74-82-8; CH_3CO^+, 15762-07-9; $CH_3^{\bullet}$, 2229-07-4; $CH_2CO^{\bullet+}$, 64999-16-2; D_3CCOCH_3, 7379-29-5; H_3CCHO, 75-07-0; CD_3I, 865-50-9; $D_3CCH(O^-)CH_3$, 142465-08-5.

(49) Holmes, J. L.; Burgers, P. C.; Mollah, M. Y. A.; Wolkoff, P. *J. Am. Chem. Soc.* **1982**, *104*, 2879.
(50) Holmes, J. L.; Burgers, P. C.; Mollah, Y. A. *Org. Mass. Spectrom.* **1982**, *17*, 127.
(51) Donchi, K. F.; Brownlee, R. T. C.; Derrick, P. J. *J. Chem. Soc., Chem. Commun.* **1980**, 1061.
(52) McAdoo, D. J.; Traeger, J. C.; Hudson, C. E.; Griffin, L. L. *J. Phys. Chem.* **1988**, *92*, 1524.
(53) Baer, S. Ph.D. Thesis, Stanford University, 1990.
(54) Osterheld, T. H. Unpublished results.

The Bromite-Iodide Clock Reaction[1]

Roberto de Barros Faria,[†] Irving R. Epstein,* and Kenneth Kustin*

Contribution from the Department of Chemistry, Brandeis University, Box 9110, Waltham, Massachusetts 02254-9110. *Received March 4, 1992*

Abstract: Clock reaction behavior has been found in the pH range 6-8 for the reaction between bromine(III) and iodide ion when the initial bromine(III) concentration exceeds one-fourth the initial iodide ion concentration. The overall stoichiometry is $2I^- + 3HBrO_2 \rightarrow 2IO_3^- + 3Br^- + 3H^+$. In this relatively fast clock reaction, a brown color due to formation of I_2 and I_3^- intensifies, reaches a peak, and then abruptly disappears. For total initial bromine(III) ($[Br^{III}]_0$) and iodide ion ($[I^-]_0$) concentrations of 8.6×10^{-4} and 5×10^{-4} M, respectively, the time to reach the peak increases from 0.23 s at pH 6 to 6 s at pH 8. After that stage of reaction, I_2 is oxidized relatively rapidly according to $2I_2 + 5HBrO_2 + 2H_2O \rightarrow 4IO_3^- + 5Br^- + 9H^+$. A secondary, smaller increase in optical absorbance occurs when $1/4 < [Br^{III}]_0/[I^-]_0 < 3/2$. The rate law has been redetermined for the process $4I^- + HBrO_2 + 3H^+ \rightarrow 2I_2 + Br^- + 2H_2O$, which initiates the clock reaction. A mechanism incorporating autocatalytic formation of HOI, in which IBr is a transient but significant intermediate, has been developed which successfully models the system's dynamical behavior in computer simulations.

Introduction

The kinetics of bromine(III) reactions acquired particular significance following the development of mechanisms to explain oscillations in the Belousov-Zhabotinsky (BZ) reaction wherein an organic species, e.g. malonic acid, is oxidized by bromate ion at high acidity in the presence of a catalyst such as Ce^{III}/Ce^{IV}.[2] Few experimental studies of bromine(III) reactions were known, however, because this oxyhalogen was not commercially available at that time, and it is unstable below pH 6-7 where the predominant Br(III) species is bromous acid, $HBrO_2$. Thus, studies of

[†] Departamento de Química Inorgânica, Instituto de Química, Universidade Federal do Rio de Janeiro, 21941 Rio de Janeiro, RJ, Brazil.

(1) Systematic Design of Chemical Oscillators. Part 81. For Part 80, see: Rábai, Gy.; Epstein, I. R. *J. Am. Chem. Soc.* **1992**, *114*, 1529.
(2) Field, R. J.; Burger, M., Eds. *Oscillations and Traveling Waves in Chemical Systems*; Wiley: New York, 1985.

0002-7863/92/1514-7164$03.00/0